COMPASS – Guiding Reconstruction with Parallel MRI Signal Structure

Yudong Zhu[1]
[1]*Zhu Consulting, Scarsdale, NY, United States*

INTRODUCTION: Recent parallel MRI methods exploit matrix properties with, e.g., low-rank matrix completion[1] and null space[2], furthering the linear relationship insights exploited with sensitivity estimates in the SENSE[3] type or with kernel determinations in the GRAPPA[4] type methods. In this work we show that one can directly identify a parallel MRI signal structure based on imaging physics, elucidate relevant rank/dimensionality with physical parameters, practice reconstruction by finding spectra/images that conform to both the signal structure and acquired spectra samples, and improve SNR by emphasizing conformity to the signal structure.

THEORY: MRI maps transverse magnetization. A spatially varying sensitivity causes a receive channel to sense an intermediate spectrum that results from a convolution of the spectrum of the transverse magnetization with the spectrum of the sensitivity. In Ξ, the spectra sensed by channels in parallel MRI, a structure is thereby embedded. This structure may be exploited through a conceptual stencil dissecting the k-space grid. As Fig.1 illustrates, for any given stencil a shift-invariant matrix $\mathbf{K}$ exists that relates samples of Ξ to samples of the magnetization's spectrum:

$$\mathbf{d}_i = \mathbf{K}\,\mathbf{x}_i\,, \quad \forall\, i \qquad (1)$$

where i is a location index for the stencil placement, $\mathbf{d}_i$ contains samples of Ξ collected by the stencil, and $\mathbf{x}_i$ contains samples of the magnetization's spectrum in a support neighborhood set by the stencil and the convolution kernels. The dimension of the column space of $\mathbf{K}$ is less or equal to the size of the support neighborhood. Eqn.1 states that vectorized signal samples belong to a signal structure space, the column space of $\mathbf{K}$. This implies a projection invariance:

$$\mathbf{d}_i = \mathbf{U}\mathbf{U}^H\,\mathbf{d}_i\,, \quad \forall \mathbf{d}_i \qquad (2)$$

where columns of matrix $\mathbf{U}$ are orthonormal basis vectors for $\mathbf{K}$'s columns.

COMpletion with **P**arallel **A**cquisition **S**ignal **S**tructure, or **COMPASS**, reconstructs multi-channel spectra from an under-sampled version acquired by parallel receive. A signal structure space is first identified from available samples of Ξ and is then applied to reconstruct Ξ in full.

Identification principle: When supported by available samples of Ξ, a $\mathbf{U}$ can be obtained through QR or SVD of matrix $[\mathbf{d}_1\ \mathbf{d}_2\ \dots\ ]$ that is assembled from known $\mathbf{d}_i$'s. In the presence of measurement noise it is useful to assemble more $\mathbf{d}_i$'s than the dimension of the signal structure space and to retain only basis vectors that correspond to significant singular values.

Reconstruction principle: In a k-space sweep, at each step the stencil assembles samples, acquired or unknown, and constrains, with Eqn.2, the resulting vector to be in the identified signal structure space. The projection operator $\mathbf{U}\mathbf{U}^H$ is shift-invariant. Applying Eqn.2 everywhere can thus be converted into an equivalent set of constraints in convolution form and further, with Fourier transform, into a rapidly quantifiable set of constraints on the individual channel images:

$$\begin{cases} \boldsymbol{y}^{(1)} = \boldsymbol{W}^{(1,1)} \times \boldsymbol{y}^{(1)} + \boldsymbol{W}^{(1,2)} \times \boldsymbol{y}^{(2)} + \dots + \boldsymbol{W}^{(1,N)} \times \boldsymbol{y}^{(N)} \\ \vdots \\ \boldsymbol{y}^{(N)} = \boldsymbol{W}^{(N,1)} \times \boldsymbol{y}^{(1)} + \boldsymbol{W}^{(N,2)} \times \boldsymbol{y}^{(2)} + \dots + \boldsymbol{W}^{(N,N)} \times \boldsymbol{y}^{(N)} \end{cases} \qquad (3)$$

In Eqn.3 weighted sums of $\mathbf{y}^{(n)}$'s, the individual channel images, are formed using $\mathbf{W}^{(m,n)}$'s, spatial weighting profiles calculated from $\mathbf{U}$. In parallel MRI it is neither possible nor necessary to unambiguously resolve $\mathbf{K}$ or sensitivity profiles. Transformed from Eqn.1, the convolution form or the weighted superposition form expresses the signal structure constraints due to imaging physics without involving other assumptions. These constraints, along with constraints due to the measured, under-sampled spectra, form a set of linear equations:

$$\begin{bmatrix} \alpha(\mathbf{I}-\mathbf{W}) \\ (\mathbf{I}-\boldsymbol{\Omega})\,\mathbf{F} \end{bmatrix}\mathbf{y} = \begin{bmatrix} \mathbf{0} \\ \mathbf{b} \end{bmatrix} \qquad (4), \quad \text{or, alternatively,} \quad \begin{bmatrix} \alpha(\mathbf{I}-\mathbf{W})\,\mathbf{F}^{-1} \\ \mathbf{I}-\boldsymbol{\Omega} \end{bmatrix}\mathbf{z} = \begin{bmatrix} \mathbf{0} \\ \mathbf{b} \end{bmatrix} \qquad (5)$$

where $\mathbf{y}$ pools $\mathbf{y}^{(n)}$'s, $\mathbf{z}$ pools the channels' spectra, matrix $\mathbf{F}$ and $\mathbf{F}^{-1}$ represent Fourier and inverse Fourier transforms respectively, $\mathbf{b}$ collects sample data acquired by parallel receive, and diagonal matrix $(\mathbf{I}-\boldsymbol{\Omega})$ represents the sampling with 0's and 1's. A least-squares solution to either set leads to reconstruction of Ξ, and individual and combined images. The two, in explicit optimization forms, readily accommodate regularization / other models, e.g., a sparse model. For instance:

$$\text{argmin}_{\mathbf{y}}\ \alpha^2\|(\mathbf{I}-\mathbf{W})\,\mathbf{y}\|_2^2 + \|(\mathbf{I}-\boldsymbol{\Omega})\mathbf{F}\,\mathbf{y}-\mathbf{b}\|_2^2 + \text{penalty term(s) based on additional model(s)} \qquad (6)$$

Impact of measurement noise on reconstruction is mediated by the two distinct sets of constraints. Scalar α can be set to emphasize the more reliable one of the two to benefit image SNR. A robust scheme for structure identification may make the first set very reliable. Then choosing a large α is helpful, and one can analytically track noise propagation, predict image noise standard deviation and possibly introduce further optimization.

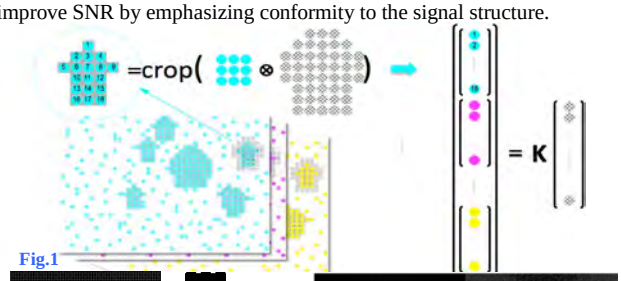

Fig.1

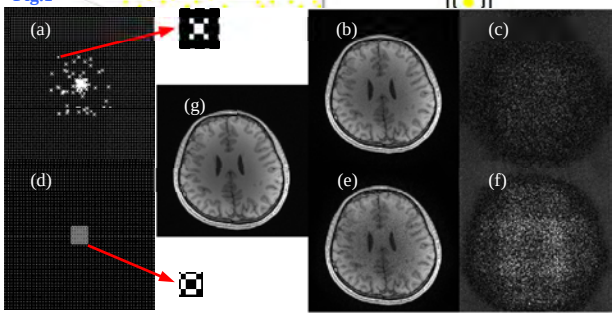

Fig.2 (g) full-sampling reference, (a) 8.7x under-sampling pattern and 8-point stencil, (b) COMPASS result, and (c) difference x10; (d-f) a case with a 15.1x under-sampling pattern and 8-point stencil.

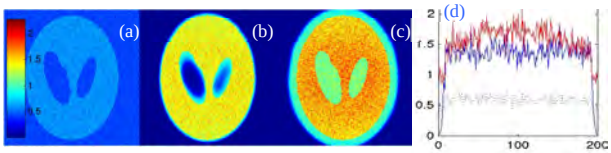

Fig.3 Measured image noise stddev profiles: (a) full-sampling s.o.s. reference, (b) COMPASS, (c) ESPIRiT, and (d) reference (black), COMPASS (blue) and ESPIRiT (red), along the mid vertical line.

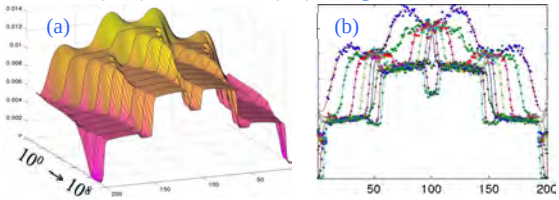

Fig.4 Image noise stddev: (a) analytically predicted profiles shown as a function of α, (b) measured profiles (dots) additionally shown.

RESULTS: Evaluation and benchmarking studies were conducted. Comparison with ESPIRiT and GRAPPA algorithms in particular used Lustig group's *sparseMRI* package[5]. In vivo data acquired with a 32-channel coil were used in a first study. Fig.2 summarizes results from two cases. Notice the satisfactory reconstruction accuracy despite a lack of center k-space full sampling. SNR in the 15.1x case is lower than that in the 8.7x case, as expected.

A second study evaluated SNR behaviors with simulations. In one case 8-channel parallel MRI employed 4x k_x-k_y under-sampling to accelerate data acquisition. The sampling pattern covered, with full-sampling for calibration, a center 24x24 block of the k_x-k_y grid, and, with random under-sampling, the rest of the grid. In each experiment, the original parallel MRI data samples, after corrupted with simulated measurement noise and under-sampled with the sampling pattern, were used as input to COMPASS (with α set to 300 in Eqn.5), ESPIRiT and GRAPPA. Profiles of image noise standard deviation were estimated from repeating the experiment 100 times. Results suggest that in this case the three methods had similar accuracy, yet differed significantly in noise standard deviation (Fig.3). When averaged over the phantom, the noise standard deviation values were, respectively, 1.26, 1.52 and 1.83, giving COMPASS an SNR advantage over ESPIRiT and GRAPPA.

To study α's impact on COMPASS' SNR behavior, we additionally investigated a 1D case. The case was set up with magnetization and sensitivity profiles over a line segment in a 2D 8-channel case (similar to the one above), and with 4x even under-sampling of k-space. Owing to the size of the 1D problem the cost for computing analytical predictions of image noise standard deviation was modest. Under a setting where noise effect on structure identification was removed, the analytical predictions suggested that image noise would decrease monotonically as α increases from 10^0 to 10^8 (Fig.4). Monte Carlo simulations confirmed this, and further indicated that as the noise effect increased, image noise profiles deviated more and more from the analytical predictions starting at several discrete locations.

DISCUSSIONS: COMPASS offers a general and flexible framework for image reconstruction. It reconstructs by identifying and applying a structure space of parallel MRI signals, with a compatibility with a wide variety of sampling patterns for identification and reconstruction, and without a need for sensitivity profile estimation. It appears to be very competitive in accuracy, including in example cases with up to 128 channels and 49x under-sampling. Having a distinct set of signal structure constraints and emphasizing it as appropriate, COMPASS further allows the structure to guide or anchor the reconstruction for SNR improvement without a cost to accuracy. COMPASS accommodates other models/constraints such as regularization and sparseness models, as some of our additional examples demonstrated.

1.Lustig, et al *Proc ISMRM* pp.483, 2011. 2.Zhang, et al *MRM* 66:1241-53, 2011. 3.Pruessmann, et al *MRM* 42:952-62, 1999. 4.Griswold, et al *MRM* 47:1202-10, 2002.